Electron transport in impulsive SEP events

LI, G.[1,2], WANG, L. AND LIN, R. P.
[1] *Space Science Lab, University of California, Berkely, CA 94720*
[2] *IGPP, University of California, Riverside, CA 94521*
ganli@ssl.berkeley.edu

Abstract: Impulsive solar energetic particle (SEP) events often show a high e/p ratio and over-abundance of He3. The underlying acceleration mechanism of particles (electrons and ions) in these events is still unknown. One crucial step in advancing our understanding of the acceleration process is to deduce precisely the injection time of electrons and ions from the observed time-intensity profiles and particle spectra at 1 AU. As such, a detailed transport model is needed. Recently, we developed a Monte-Carlo model to follow electron transport in an impulsive SEP event. In a collisionless plasma like the solar wind, the propagation of electrons follows the Parker Spiral field lines with little pitch angle scattering that is caused by the presence of solar wind turbulence. The effect of the pitch angle scattering is to alter the pitch angles of particles in a random manner. By casting the governing Fokker-Planck equation to a set of equations describing the motion of individual particle, we obtain the time intensity profile, the pitch angle distribution and its time evolution. Using the model, two example impulsive events from WIND 3DP measurements are studied. The injection times of electron are obtained by fitting the observed time intensity profiles and pitch angle distributions as a function of time. These injection times provide crucial clues to understand the underlying acceleration process.

Introduction

An mpulsive SEP event is often dominated by $\sim 1-100$ keV electrons and low energy, $\sim 0.01-10$ MeV/nuc ions that are highly enriched in ^3He. the $^3He/^4He$ ratio in these events can go up to 30, a factor up to 10^5 increase over the normal coronal value [2]. Many impulsive events also show enhancements of various high-charge-state heavy ions such as Fe and trans-iron with mass up to 220 amu [6, 3]. In these impulsive events, there are close associations between non-relativistic electrons and ^3He. The strong enhancements of ^3He in impulsive events have attracted many theoretical explanations. For example, [8] and [7] suggested that oblique electromagnetic ion cyclotron waves (EMIC waves) can efficiently energize ^3He and a subset of heavy elements, depending on their Q/M ratios. [5] have investigated stochastic acceleration of ^3He and ^4He by EMIC waves propagating parallel to the magnetic field. [4] discussed acceleration of ^3He by firehose instability due to electron temperature anisotropy. These theories have attempted to link the acceleration of electron and ^3He one way or another. To prove or disprove these theories, it is crucial to obtain accurate injection profiles of both electrons and ions at the Sun, which requires a good understanding of the transport of both electrons and ions in the interplanetary medium.

In this pape we study the pitch angle scattering effects on the propagation of energetic electrons. We adopt a Monte-Carlo approach to solve the transport equation. We first translate the underlying Fokker Planck equation to a set of equations describing single particle's motion. The motion is decomposed into a *deterministic* part and a *stochastic* part. The *deterministic* part describes the motion of electron in a prescribed magnetic field (Parker spiral in this case), and the *stochastic* part describes the diffusion of particle's pitch angle due to the weak turbulence in the solar wind. Using this approach, we study two example events, the 1998 August 29 event and the 2002 October 20 event.

Electron transport with weak pitch angle scatterings

To facilitate a Monte-Carlo simulation, one first decompose single particle motion of an electron to the follow equations [1].

$$\frac{dz}{dt} = \mu v \quad (1)$$

$$\frac{d\mu}{dt} = \frac{v}{2}\frac{1-\mu^2}{L}. \quad (2)$$

$$\tilde{d\alpha} = sign(\xi' - 1/2) erf^{-1}(\xi)\sqrt{4D_0|\mu|^{q-1}dt} \quad (3)$$

$$\frac{dp'}{dt} = \frac{p'U^{sw}}{-r}[\frac{\mu^2 sin^2\Phi}{csec\theta} + \frac{1-\mu^2}{2}(1+\frac{cos^2\Phi}{csec\theta}) \quad (4)$$

where we assume the IMF is given by the Archimedean spiral,

$$B_r = B_0(\frac{R_0}{r})^2, \quad (5)$$

$$B_\theta = 0, \quad (6)$$

$$B_\phi = B_r\frac{\Omega_0 r sin(\theta)}{u^{sw}} \qquad \text{where} \qquad r >> R_0 \quad (7)$$

Now one can follow the propagation of individual particles. The time intensity profile and pitch angle distribution at 1 AU are obtained by summing over all single particle instances.

Modeling the 2002 October 20 event

Using the technique developed in the last section, we model one impulsive SEP event, the 2002 October 20 event. We chose this event because 1) its clean background (high signal to noise ratios) and 2) its symmetric triangular profiles at high energies. A clean background is crucial for our study. In particular, one would like to minimize the probability of multiple injections at the Suns, which adds another complication to the study. To that end, one could also use the associated X-rays and Type III radio bursts as indicators of multiple (or the lack of) injections. We also follow our earlier practice by selecting events which show symmetric triangular profiles at high energies [9]. This allow us to use a symmetric angular injection profile. In future work, we plan to relax this selection criterion and study events having asymmetric time intensity profiles using a Reid-Axford type injection profile [*Reid*, 1964].

Figure 1 and 2 plot the time evolution of the PAD for the 180 keV and 690 eV channels. The upper panels show the observed time intensity profiles (black curves) versus those from fitting (red curves). The second panels plot the observed and simulated PAD width; PAD width is calculated by taking the difference between α_{center} and $\alpha_{1/2}$; with α_{center} the pitch angle where the electron flux is the highest and $\alpha_{1/2}$ the pitch angle where the electron flux drops to half of its maximum value. The third panels plot the observed spectrogram of PAD and the forth panels are our simulation results. From the second panels of the figure, we can see that at 690 eV, the pitch angle width is initially $\sim 25^\circ$ (which is limited by the instrument resolution $\sim 22.5^\circ$), and remains relatively constant during the rising phase and early decay phase of the event. In the late decay phase, however, the pitch angle width increases, reflecting a more isotropic distribution of the pitch angle. The red curves in the figure is the simulated pitch angle width. We find a very good agreement between the simulation and the observation. At 180 keV, the observed PAD width quickly reaches $70^\circ - 80^\circ$ and increases to $\sim 90^\circ$ at the slow decay phase. In comparison, the pitch angle width from simulation is smaller, changing from an initial $\sim 30^\circ$ to about 50° at the peak of the event and only reaches $\sim 90^\circ$ in the slow decay phase. This difference is also evident in the spectrogram of PADs from the 3rd and 4th panels. The 3rd and 4th panels of figure 1 and figure 2 are the evolutions of PAD. The fluxes are shown in log scale and color coded. At 690 eV, the simulated PAD evolution agree very well with the observations. At 180 keV, however, the simulation (4th panel) shows fewer electrons having large pitch angle at the peak comparing to the observation (3rd panel). Furthermore, the observation shows that the pitch angle decreases almost immediately from 180° to $< 50^\circ$ at the onset, while the simulation shows a more gradual decrease of PA at the onset (recall that the magnetic field is pointing toward the Sun and $\alpha = 180^\circ$ is point outward against the magnetic field). This means that near 1 AU, at higher energies, the pitch angle scattering effect from the observation is stronger than that obtained from the simulation.

We also plot the derived triangular injection profiles for these two events in figure 3. In an earlier

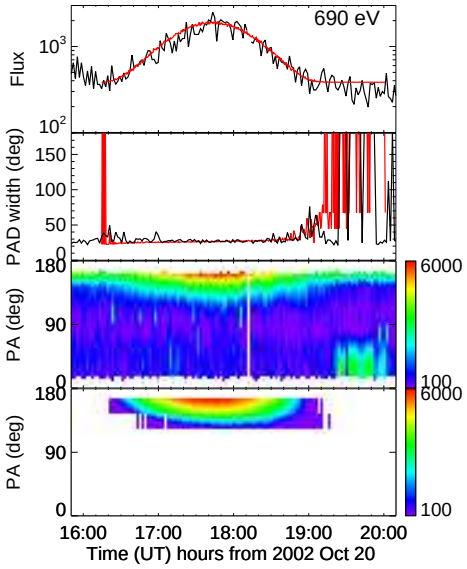

Figure 1: Evolution of pitch angle distribution for the 2002 October 20 event at $T = 690$ eV The first panels show the time intensity profiles. The second panels plot the PAD width. The third panels plot the color-coded spectrogram of the observed PADs and the forth panels are the corresponding simulation results. See text for details.

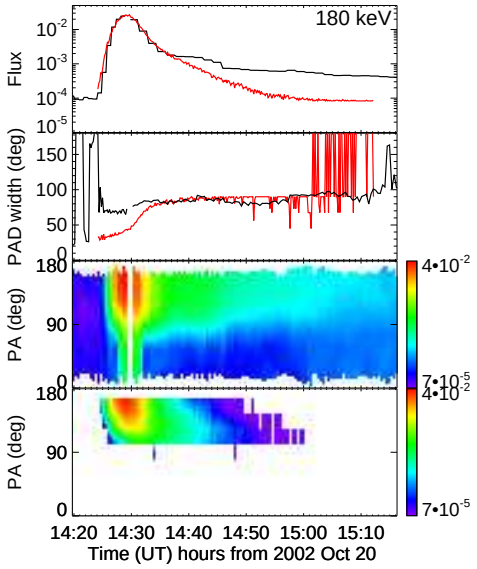

Figure 2: Evolution of pitch angle distribution for the 2002 October 20 event at $T = 180$ keV The first panels show the time intensity profiles. The second panels plot the PAD width. The third panels plot the color-coded spectrogram of the observed PADs and the forth panels are the corresponding simulation results. See text for details.

study, by assuming "free streaming" of electrons, [*Wang et al,* 2005] surveyed 12 events and found that the injection duration for low energy electrons can last over an hour. In the current study, we include the pitch angle scattering. We still find relatively long duration for the low energy electron injections. Indeed, for the ~ 710 eV electrons, we find the duration for the 2002 October 20 event to be 2.1 hours. At higher energies, the injection duration becomes smaller. For 310 keV electrons, the duration is 6 minutes. It is interesting to compare the electron injection start times with type III radio bursts, which are indicated by the dashed vertical lines in figure 3. From the figure, it is clear that the type III radio bursts occur *after* the injection start-times of low energy electrons and *before* those of high energy electrons, agree with earlier studies [*Krucker et al*, 1999; *Haggerty and Roelof*, 2002]. This sequence of first low energy electron injections, followed by type III radio bursts and then high energy electron injections, is in agreement with the scenario where electrons are *continuously* accelerated by certain process, and during their acceleration, they excite type III bursts while at the same time are further accelerated to higher energies.

If indeed the high energy electrons are of the same source as the lower energy electrons, one can estimate the acceleration time t_{acc}, which is roughly the difference between the injection start-times of low energy electrons and that of high energy electrons. We find $t_{acc} \sim 25$ minutes from 0.4 keV to 510 keV. Recently, *Wang et al* [2006b] reported that jet-like features are observed in small ^3He-electron rich impulsive events. These jets are typically ejected out at the boundaries of active regions with a speed of several hundred km/s. Assuming these jets are the acceleration sites for the high energy electrons (e.g. through first order Fermi acceleration), a $20-30$ minutes duration will translate to

a distance of $1-2R_{\odot}$, consisting with the scenario that the jet is accelerating electrons (and possibly ions) within several $r_{\odot}$'s.

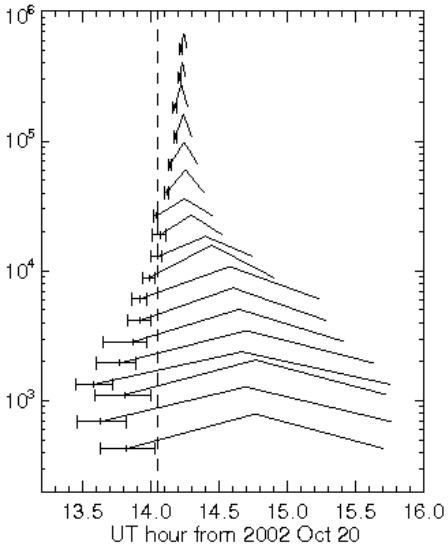

Figure 3: The injection profiles for the 2002 October 20 e vent (right). The duration of the injections are shown as the triangles. The uncertainties of the start-times, estimated from fitting, are shown as the error bars. The vertical dashed lines indicate the onset time of the type III radio bursts.

Conclusion

To summarize, we have developed a Monte-Carlo approach to investigate the transport of electrons in small impulsive events where pitch angle scattering is weak. We model the pitch angle scattering as a *stochastic* process, where an electron's pitch angle is changed *continuously* due to the presence of the interplanetary magnetic turbulence. By following single particle motion of individual electrons from the Sun to 1 AU, we construct both the time intensity profiles and the time evolution of electron PADs. Fitting to one particular event is shown where the time intensity profiles and the evolution of PADs are presented. We also obtain both the injection profiles of electrons at the Sun. We find the injection duration for low energy electrons are much longer ($\sim$ 2 hours at $\sim$ 700 eV) than high energy electrons ($\sim$ 6 minutes at $\sim$ 200 keV). Furthermore, the low energy electrons are injected earlier than high energy electrons.

Acknowledgements

The authors acknowledge the partial support of NASA grants NNG05GM62G and NAG5-10932 for GL and NASA grant NNG05GH18G for LHW and RPL.

References

[1] G. Li, L. Wang, and R. P. Lin. On electron transport in impulive sep events – understanding wind observations. *submitted to JGR*, 2007.

[2] G. M. Mason, J. R. Dwyer, and J. E. Mazur. New properties of 3he-rich solar flares deduced from low-energy particle spectra. *Astrophy. J.*, 545:L157, 2000.

[3] G. M. Mason, J. E. Mazur, J. R. Dwyer, J. R. Jokipii, R. E. Gold, and S. M. Krimigis. Abundances of heavy and ultraheavy ions in 3he-rich solar flares. *Astrophy. J.*, 606:555, 2004.

[4] G. Paesold, R. Kallenbach, and A. O. Benz. Acceleration and enrichment of 3he in impulsive solar flares by electron firehose waves. *Astrophy. J.*, 582:495, 2003.

[5] V. Petrosian and S.M. Liu. Stochastic acceleration of electrons and protons. i. acceleration by parallel-propagating waves. *Astrophy. J.*, 610:550, 2004.

[6] Donald V. Reames. Abundances of trans-iron elements in solar energetic particle events. *Astrophy. J.*, 540:L111, 2000.

[7] I. Roth and M. Temerin. Enrichment of 3he and heavy ions in impulsive solar flares. *Astrophy. J.*, 477:940, 1997.

[8] M. Temerin and I. Roth. The production of he-3 and heavy ion enrichment in he-3-rich flares by electromagnetic hydrogen cyclotron waves. *Astrophy. J.*, 391:L105, 1992.

[9] L. Wang, R. P. Lin, S. Krucker, and G. M. Mason. A study of the solar injection for eleven impulsive electron/3he-rich sep events. *SW11 proceedings*, 16:457, 2005.